Strojniški vestnik - Journal of Mechanical Engineering 55(2009)10, 575-580
UDC 531.715

Paper received: 07.06.2009
Paper accepted: 25.09.2009

Homodyne Quadrature Laser Interferometer Applied for the Studies of Optodynamic Wave Propagation in a Rod

Tomaž Požar* - Janez Možina
University of Ljubljana, Faculty of Mechanical Engineering, Slovenia

The localized Coulomb dry friction on the surface of a rod significantly alters the propagation of an optodynamic wave. The effects of frictional clamping on the rod's dynamics were measured with a homodyne quadrature laser interferometer at the rear end of the rod. The measurements are supported by a theoretical description of the discrete motion of the finite rod, which is based on a general result representing the interaction of a laser-ablation-induced stress wave with a frictional clamping location.

Keywords: optodynamics, homodyne quadrature laser interferometer, wave propagation, friction

0 INTRODUCTION

In an earlier paper we described the formation of an optodynamic wave as well as its propagation and multiple reflections from both faces of an unclamped finite rod [1]. We observed that ablation of the front face of a rod using a nanosecond laser pulse induces a short stress wave - an optodynamic wave - that propagates and reverberates inside the rod. However, if the rod is locally clamped, the wave discretely transfers its initial linear momentum as it impinges on the clamping location multiple times. The momentum transfer to the clamping was determined by measuring the axial displacement of the rear end of the rod.

In order to monitor the motion of the rear end of the rod over its several micrometer long path, we had to develop an interferometric method based on quadrature detection [2]. This contactless displacement-measuring instrument, a homodyne quadrature laser interferometer (HQLI), enables high dynamic range, single shot measurements of abrupt high-amplitude ultrasound superimposed on moving objects with a sub-nanometer resolution.

This paper explains general effects on the rod's dynamics caused by the presence of the localized Coulomb dry friction. Such effects need to be taken into account in various fields, for example, ablative laser propulsion [3], split-Hopkinson pressure-bar (SHPB) experiments [4] dynamic behavior of frictional contacts [5], and friction studies on the nanoscale [6].

1 THEORY

In order to determine what occurs to the incident compressional stress wave when it impinges on the clamping location, consider a semi-infinite rod, as illustrated in Fig. 1, setting $L \to \infty$. The rod is circular, elastic, homogeneous and isotropic, has the length L, cross-section A, Young's modulus E, density ρ, and longitudinal acoustical impedance $Z = \rho c_0$. A t_p = 10-ns Nd-YAG pulse ablates its front face at $x = 0$ and induces a $c_0 t_p$ - long optodynamic wave propagating with the speed $c_0 = \sqrt{E/\rho}$. The rod is point-clamped at $x = x_0$ with a variable contact normal force F_N. Except at the clamping location, the rod has stress-free surfaces. Three displacements of interest are drawn: the end of the rod, u_e, the clamping position, u_c, and the center of mass, u^*.

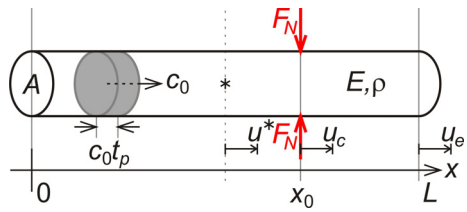

Fig. 1. *Basic parameters of the rod*

To explain the interaction and the wave's dynamics theoretically we set a suitable linearized form of the elementary wave equation for a rod [7] and [8], including point-like, Coulomb dry-friction forces on the surface circumference at $x = x_0$, as

*Corr. Author's Address: University of Ljubljana, Faculty of Mechanical Engineering, Aškerčeva 6, 1000 Ljubljana, Slovenia, tomaz.pozar@fs.uni-lj.si

$$\frac{\partial^2 u(x,t)}{\partial x^2} = \frac{1}{c_0^2}\frac{\partial^2 u(x,t)}{\partial t^2} + \\ + \frac{I_F}{E}\delta(x - x_0)\delta(t - x_0/c_0). \quad (1)$$

Here, the clamping is understood to be incompressible and localized, and, therefore, the friction forces are assumed to be concentrated and can be represented by a delta function. $u(x,t)$ represents the axial displacement at any given point x and time t; $v(x,t)$ is the corresponding particle velocity; and $\sigma(x,t)$ is the stress.

The passage of the wave under the clamping gives rise to a pressure impulse exerted by frictional forces $I_F = \int P_F(t)dt = p_c/A$ that equals the momentum acquired by the clamping p_c, divided by A. In this specific case, I_F can also be expressed in terms of the coefficient of friction between the rod and the clamping, μ, the normal force, F_N, and the time needed for the wave to cross the clamping location, t_c, as $I_F = \mu F_N t_c/A$. The nanosecond laser ablation of the front face of the rod can be modeled by a boundary-loading condition [9] and [10], $\sigma(0,t) = -I_A\delta(t)$. Similar to I_F, $I_A = \int P_A(t)dt = p_0/A$ represents an ablation pressure impulse that equals the momentum p_0 obtained by the rod due to the laser-pulse ablation divided by A. The initial duration of the optodynamic wave, t_c, equals [3] and [11] the laser-pulse duration, t_p. If the dispersion [9] is neglected, $t_p = t_c$, otherwise $t_p < t_c$. I_A can be approximated by $P_0 t_p$, where P_0 describes the constant normal pressure acting evenly on the front plane of the rod during the laser ablation.

Eq. (1) can be solved using standard one-sided Laplace-transformation methods [12]. The rod is initially undisturbed $u(x,0) = 0$ and at rest $v(x,0) = 0$. Taking into account the initial and boundary loading conditions and including the requirement $u(x \to \infty, t) = 0$, we obtained the following solution of Eq. (1) in a dimensionless form composed of Heaviside unit-step functions. The solution for a displacement is presented in terms of the forward- and backward-propagating waves.

$$\tilde{u}(\tilde{x},\tilde{t}) = \left[1 - \frac{\tilde{I}}{2}\mathrm{H}(\tilde{x} - \tilde{x}_0)\right]\mathrm{H}(\tilde{t} - \tilde{x}) + \\ + \left[-\frac{\tilde{I}}{2} + \frac{\tilde{I}}{2}\mathrm{H}(\tilde{x} - \tilde{x}_0)\right]\cdot \\ \cdot\mathrm{H}(\tilde{t} + (\tilde{x} - 2\tilde{x}_0)) + \\ + \left[-\frac{\tilde{I}}{2}\right]\mathrm{H}(\tilde{t} - (\tilde{x} + 2\tilde{x}_0)) \quad (2)$$

For the sake of compactness, the following dimensionless variables, designated by the tilde, are introduced:

$$\tilde{x}_\alpha = \frac{x_\alpha}{L}, \quad \tilde{t}_\alpha = \frac{t_\alpha}{t_L} = \frac{t_\alpha}{L/c_0}, \\ \tilde{I} = \frac{I_F}{I_A} = \frac{\mu F_N t_c}{ZAu_0}, \quad \tilde{u}_\alpha = \frac{u_\alpha}{u_0} = \frac{u_\alpha}{I_A/Z}, \\ \tilde{v}_\alpha = \frac{v_\alpha}{u_0/t_p}, \quad \tilde{p}_\alpha = \frac{p_\alpha}{p_0} = \frac{p_\alpha}{ZAu_0}, \\ \tilde{\sigma}_\alpha = \frac{\sigma_\alpha}{I_A/t_p}, \quad \tilde{\mathrm{E}}_\alpha = \frac{E_\alpha}{E_0} = \frac{E_\alpha}{ZAu_0^2/t_p}. \quad (3)$$

α can be substituted by any suitable symbol-string index or * in the superscript that denotes the center of mass. u_0 is a measurable quantity [1] equal to one half of the displacement caused by the reflection of the wave from the rear end of the unclamped rod (see Fig. 3). p_0 is the momentum carried by the primary wave and E_0 is its total mechanical energy, consisting of equal contributions from the kinetic and elastic parts.

The first term on the right-hand side of Eq. (2) corresponds to the forward-propagating wave with its origin at $\tilde{x} = 0$. The value inside the square brackets is the displacement of the rod's cross-section once it has been traversed by the wave. In the region $0 < \tilde{x} < \tilde{x}_0$ it is termed the *incident* wave, and for $\tilde{x}_0 < \tilde{x}$ the *transmitted* wave. The second term corresponds to the backward wave, starting at $\tilde{x} = 2\tilde{x}_0$. In the region where the value in the square brackets is nonzero, i.e., for $0 < \tilde{x} < \tilde{x}_0$, the wave corresponds to the *reflected* wave. The third term is of lesser

Table 1. *Properties of the clamping and the waves before and after the interaction with a point-like frictional location in a concise lookup-table form*

	no fiction				kinetic friction				static friction			
	$\tilde{I}=0$				$0<\tilde{I}<2$				$\tilde{I}=2$			
location	$\tilde{u}$	$\tilde{v}$	$\tilde{\sigma}$	$\tilde{p}$	$\tilde{u}$	$\tilde{v}$	$\tilde{\sigma}$	$\tilde{p}$	$\tilde{u}$	$\tilde{v}$	$\tilde{\sigma}$	$\tilde{p}$
incident wave	1	1	−1	1	1	1	−1	1	1	1	−1	1
transmitted w.	1	1	−1	1	$1-\tilde{I}/2$	$1-\tilde{I}/2$	$-\left(1-\tilde{I}/2\right)$	$1-\tilde{I}/2$	0	0	0	0
reflected w.	0	0	0	0	$-\tilde{I}/2$	$-\tilde{I}/2$	$-\tilde{I}/2$	$-\tilde{I}/2$	−1	−1	−1	−1
clamping loc.	1			0	$1-\tilde{I}/2$			$\tilde{I}$	0			2

importance, and corresponds to the rebound of the reflected wave at the rod's free end. Note that the frictional term in Eq. (1) is simplified in such a manner that the friction acts only once, neglecting later reverberations of the reflected wave in the region $0<\tilde{x}<\tilde{x}_0$.

Differentiating Eq. (2) with respect to $\tilde{t}$ or $\tilde{x}$ yields the corresponding particle velocity $\tilde{v}$ and stress $\tilde{\sigma}$, respectively. The expressions for $\tilde{v}$ and $\tilde{\sigma}$ are composed of delta functions, which can be approximated by suitable rectangular pulses of a length equal to $c_0 t_p$. It can also be inferred from Eq. (2) that $\tilde{I}=0$ corresponds to no friction. If $0<\tilde{I}<2$, slippage occurs and the friction is *kinetic*, and if $\tilde{I}=2$, the friction is *static*, there is no slippage and only in this case does the frictional force drop from its maximum kinetic value in order to satisfy the condition $I_F=2I_A$. The values of $\tilde{u}$, $\tilde{v}$, $\tilde{\sigma}$, and $\tilde{p}$ for the incident, transmitted, and reflected waves and for the clamping location in the three frictional regimes are gathered in Table 1. $\tilde{u}$ is a displacement of the cross-section after the passage of the wave, $\tilde{v}$ and $\tilde{\sigma}$ are the particle velocity and stress within a wave, and $\tilde{p}$ is the momentum carried by the wave or the momentum transferred to the clamping. A negative value of $\tilde{\sigma}$ corresponds to a compression.

In the static friction case, the clamping location has identical effects on the wave propagation as a fixed rod-end termination, with its characteristic velocity reversal and double wave-momentum transmission to the rigid clamping. If the friction is kinetic, the incoming compressional wave is both transmitted and reflected as a compression. The clamping receives the required momentum to satisfy the conservation-of-momentum law. This momentum is independent of the magnitude of the incoming wave if the friction is kinetic, but it is strongly dependent if the friction is static.

In the presence of slippage the energy is dissipated and the work is done by the non-conservative Coulomb dry-friction forces. The work equals the constant frictional force times the displacement of the clamping. This friction work $\tilde{W}_F=W_F/E_0=\tilde{I}(1-\tilde{I}/2)$ must also obey the work-energy theorem, and, therefore, be equal to the change of mechanical energies of the incident wave before, and the sum of the transmitted and reflected wave after, the interaction with the clamping. It achieves a maximum value when $\tilde{I}=1$.

2 EXPERIMENTAL SETUP

The experimental setup is shown in Fig. 2. The optodynamic wave was induced by a Q-switched Nd:YAG operating at 1064 nm capable of producing 10-ns-long pulses with the maximum energy of 100 mJ. The excitation laser pulse was focused to a 0.5-mm-diameter spot on the center of the front plane of a steel (AISI: 304) solid cylindrical 12-cm-long and 2-mm-thick rod.

The effects of the clamping were measured at the rear end of the rod by monitoring the axial displacement of the rear cross-section. This displacement is caused by the reflections of friction-effected mechanical compressions and rarefactions. The out-of-plane displacement was measured with a homodyne quadrature laser interferometer whose operation is described in detail in [2].

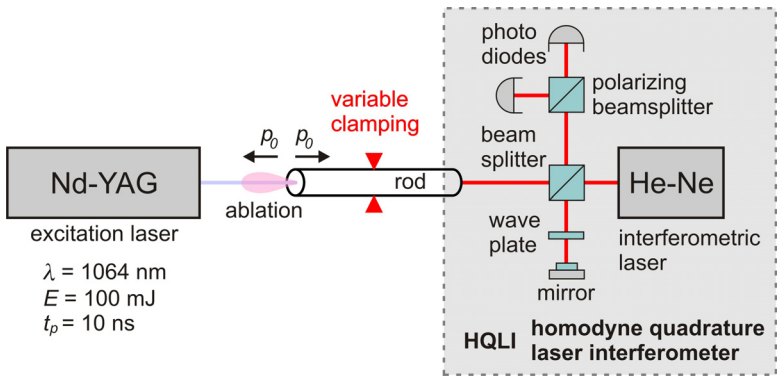

Fig. 2. *Schematic diagram of the experimental system*

3 RESULTS AND DISCUSSION

So far we have considered the first transit of the optodynamic wave over the dry-frictional clamping. Following multiple reflections and transitions of the branching waves at the clamping location, according to the results summarized in Table 1, we obtained a discrete temporal evolution of the dynamics of a *finite* rod with a localized Coulomb dry friction. The measurement of the rear-end displacement of a laser-ablated rod that is point-clamped in the middle by a variable contact force is shown in Fig. 3.

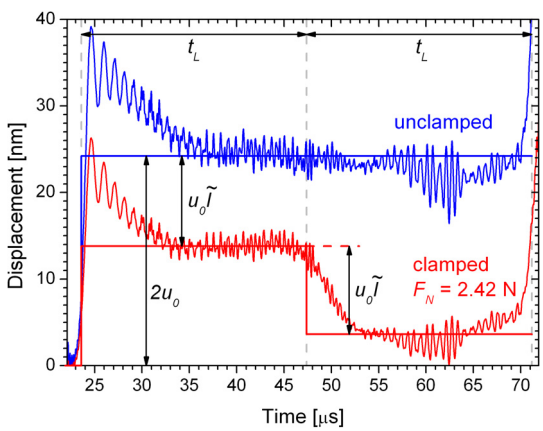

Fig. 3. *Axial displacement measured at the rear end of the 120-mm-long and 2-mm-thick steel rod as a function of time. Two displacement curves are shown: the unclamped rod and the rod clamped at its middle by a normal force of 2.42 N. From the two measurements the friction parameter of the clamped rod can be estimated to be* $\tilde{I} = 0.85$

One of the conclusions of such reasoning is that once a wave within a finite rod is reflected at the fixture, it will not pass the clamping location again. It will echo back and forth, on either one side or the other of the clamping. The only process that enables the wave to pass over the clamping location again is the interference of two or more waves, simultaneously interacting with the clamping.

In the case of weak friction $0 < \tilde{I} << 1$, the results are in accordance with the motion of a rigid body under the influence of constant deceleration due to the Coulomb friction. Even though the motion of the weakly clamped rod is discrete, its general envelope can be approximated by a smooth function. The rod slips over the clamping location by a terminal length $\tilde{u}_{c,\infty} = 1/\tilde{I}$, and the time needed for this slippage is $\tilde{t}_f = 2/\tilde{I}$. The rod's momentum and the velocity of the center of mass both decrease linearly with time

$$\tilde{p}(\tilde{t}) = \tilde{v}^*(\tilde{t}) = \begin{cases} 1 - \tilde{t}/\tilde{t}_f, & 0 \le \tilde{t} \le \tilde{t}_f \\ 0, & \tilde{t}_f < \tilde{t} \end{cases} . \qquad (4)$$

The displacement of the center of mass reaches its maximum value $1/\tilde{I}$ quadratically

$$\tilde{u}^*(\tilde{t}) = \int_0^{\tilde{t}} \tilde{v}^*(\xi) d\xi = \begin{cases} \tilde{t}\left(1 - \tilde{t}/2\tilde{t}_f\right), & 0 \le \tilde{t} \le \tilde{t}_f \\ \tilde{t}_f/2, & \tilde{t}_f < \tilde{t} \end{cases} . \qquad (5)$$

$\tilde{t}_f$ is the time needed to achieve the total slippage or the characteristic time of the

momentum transfer from the rod to the clamping as a result of the localized Coulomb dry friction. It can be estimated indirectly according to the relationship $\tilde{t}_f = 2\tilde{u}_{c,\infty}$ by measuring the total slippage. When the normal force equals the rod's weight, t_f must be smaller than $2u_0/(\mu g t_p)$, where g is the acceleration due to gravity. This type of external friction was identified in the measurements of the geometrical dispersion effects on the optodynamic wave during its multiple transitions in a finite rod [9], where $t_f < 0.5$ s and $u_{c,\infty} < 0.2$ mm were assessed according to the above estimate.

A portion of the wave's momentum is also transferred to the surrounding atmosphere on each reflection at the front and rear ends of the rod at normal air pressure. This acoustic-impedance mismatch effect leads to an exponential transfer of the rod's momentum to the air in the form of sound. $\tilde{p}(\tilde{t}) = \exp(-\tilde{t}/\tilde{\tau})$, where $\tau = t_L\tilde{\tau} = t_L(Z_{\text{steel}}/2Z_{\text{air}})$. The characteristic time of the momentum transfer from the rod to the surrounding air is $\tau = 1.2$ s for the rod in reference [9], and is of the same order as t_f.

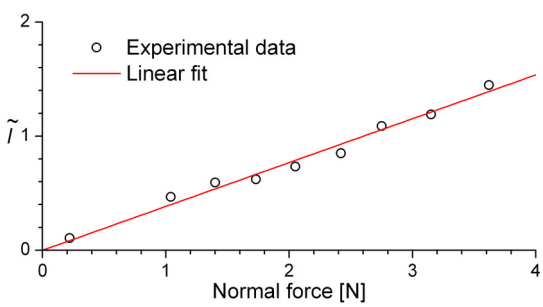

Fig. 4. *Linear dependence of the frictional parameter $\tilde{I}$ as a function of the normal force F_N*

We measured the characteristic non-dimensional parameter of the relative friction strength $\tilde{I}$ using a homodyne quadrature laser interferometer in two distinct, contactless ways. In the weak-friction regime we deduced $\tilde{I}$ from the total slippage displacement, which cannot be measured with compensated Michelson-type interferometers. On the other hand, when $\tilde{I}$ is comparable to unity, it can be determined from the ratio of the first few discrete displacements of the rod's rear end, as shown in Fig. 3. The experiments also confirm that $\tilde{I}$ is proportional to the normal force (see Fig. 4).

Our analysis of the experimental conditions employs a simple representation of the ablation and friction using delta functions. Assuming a finite stress wave and a finite clamping contact, additional effects can be expected: the wave-shape, not just the amplitude, changes after the wave's reflection from the clamping, and the residual stress distribution remains under the contacting surfaces [13], thus the rod under the clamping is pre-stressed for the subsequent arrival of the wave. We can neglect the fact that the clamping is displaced to a new location once the slippage occurs, since in our experiments the slippage is very small compared to the length of the rod. Eq. (1) assumes that the cross-sections remain plane, that the waves are not leaking from the rod to the clamping, and that the Poisson effect does not enhance the normal force [14]. Apart from the dispersion, these are the limitations of the analysis that most likely contribute to the slight dissimilarity between the theoretical prognosis and the measured curve. Based on the above-stated restrictions, it can be concluded that our description of the laser-propelled rod-movement better explains the interaction of the wave with the clamping when the friction parameter $\tilde{I}$ is smaller.

4 CONCLUSION

In conclusion, we have presented an experimentally supported description of the motion of an elastic rod that bears a localized propagating optodynamic wave and includes a stoppage mechanism in the form of the localized Coulomb dry friction. The introduced optodynamic method can also be extended to studies of nanoscale friction effects. The results can as well be applicable in a description of the structural damping of miniaturized SHPB systems.

5 REFERENCES

[1] Požar, T., Možina, J. (2008) Optodynamic description of a linear momentum transfer from a laser induced ultrasonic wave to a rod, *Appl. Phys. A, Mater. Sci. Process*. vol. 91, no. 2, p. 315-318.

[2] Gregorčič, P., Požar, T., Možina, J. (2009) Quadrature phase-shift error analysis using a homodyne laser interferometer, *Opt. express*, vol. 17, no. 18, p. 16322-16331.

[3] Anju, K., Sawada, K., Sasoh, A., Mori, K., Zaretsky, E. (2008) Time-resolved measurements of impulse generation in pulsed laser-ablative propulsion, *J. Propul. Power*, vol. 24, no. 2, p. 322-329.

[4] Jia, D., Ramesh, K.T. (2004) A rigorous assessment of the benefits of miniaturization in the Kolsky bar system, *Exp. Mech.*, vol. 44, no. 5, p. 445-454.

[5] Velkavrh, I., Kalin, M., Vižintin, J. (2008) The performance and mechanisms of DLC-coated surfaces in contact with steel in boundary-lubrication conditions - a review, *Strojniški Vestnik - Journal of Mechanical Engineering*, vol. 54, no. 3, p. 189-206.

[6] Tambe, N.S., Bhushan, B. (2005) Nanoscale friction mapping, *Appl. Phys. Lett.,* vol. 86, no. 19, p. 193102-1-193102-3.

[7] Cornelius, C.S., Kubitza, W.K. (1970) Experimental investigation of longitudinal wave propagation in an elastic rod with coulomb friction, *Exp. Mech.*, vol. 10, no. 4, p. 137-144.

[8] Nikitin, L.V., Tyurekhodgaev, A.N. (1990) Wave-propagation and vibration of elastic rods with interfacial frictional slip, *Wave Motion*, vol. 12, no. 6, p. 513-526.

[9] Požar, T., Petkovšek, R., Možina, J. (2008) Dispersion of an optodynamic wave during its multiple transitions in a rod, *Appl. Phys. Lett.*, vol. 92, no. 23, p. 234101-1-234101-3.

[10] Pan, Y., Rossignol, C., Audoin, B. (2003) Acoustic waves generated by a laser line pulse in a transversely isotropic cylinder, *Appl. Phys. Lett.*, vol. 82, no. 24, p. 4379-4381.

[11] Yang, Y.N., Yang, B., Zhu, J.R., Shen, Z.H., Lu, J., Ni, X.W. (2008) Theoretical analysis and numerical simulation of the impulse delivering from laser-produced plasma to solid target, *Chin. Phys. B*, vol. 17, no. 4, p. 1318-1325.

[12] Graff, K.F., Wave Motion in Elastic Solids, New York: Dover Publications, 1991. 649 p. ISBN 0-486-66745-6.

[13] Wilms, E.V. (1969) Damping of a Rectangular Stress Pulse in a Thin Elastic Rod by External Coulomb Friction, *J. Acoust. Soc. Am.*, vol. 45, no. 4, p. 1049-1050.

[14] Korotkov P.F. (1972) Waves in an elastic medium with coulomb surface friction present, *J. Appl. Mech. Tech. Phys.*, vol. 13, no. 4, p. 542-545.